J Solid State Electrochem (2012) 16:329–340
DOI 10.1007/s10008-011-1328-5

ORIGINAL PAPER

Characteristic simulation with various anode support thicknesses of membrane electrode assembly in SOFC

Jenn-Kun Kuo · Jian-Kai Wang

Received: 15 November 2010 / Revised: 22 January 2011 / Accepted: 30 January 2011 / Published online: 22 February 2011

Abstract This study focuses on the research of solid oxide fuel cell (SOFC) and proposes reasonably practical designs, analyses, and numerical analyses with coupling software in physics, COMSOL Multiphysics, as the analysis tool to discuss the effects on the SOFC performance. This research applies the design of electrode support (anode support) to substitute the original electrolyte support, Yttria-stabilized zirconia, so that the electrolyte membrane could form a membrane to reduce ohmic resistance and increase power density. This study further discusses the effects of various flow fields (counterflow and co-flow) on internal mass transfer and SOFC performance. The findings show that the cell performance of SOFC with co-flow is better than counterpart with counterflow under anode support thickness 1,000 μm. Regarding the analyses of porosity effect with the porosity 0.7 and tortuosity 4.5, the power density reaches the maximum that could enhance the cell performance.

Keywords SOFC · Numerical · Mass transfer · Electrolyte · Porosity · Tortuosity

Introduction

Solid oxide fuel cell (SOFC), a high-temperature fuel cell, is one of the fuel cells with the highest generating efficiency and the most varieties of fuel that it can apply hydrogen or hydrocarbon as the fuel. Besides, scheduled investment in production has helped SOFC become commercialized. Present research mainly focuses on the features of the flow fields with various anode supports and cell performance in flat SOFC and the porosity of solid oxide material in cells.

In 1994, the mathematic model of flat SOFC was the physical model based on Achenbach [1]. This study aimed to discuss the simulations of SOFC thermal current and current distributing values in various flow fields as well as the temperature distribution in the cell when SOFC transient response was simultaneously calculated. The findings showed that the design of counterflow made the temperature gradient in the cell be the largest, as the recombination reactions would absorb large amount of heat. Furthermore, the current density of co-flow was evenly distributed, and the counterflow is the best of the entire cell performance. In 1995, Achenbach [2] proceeded theoretical analyses on SOFC transients and, aiming at the demands of engineer applications, proposed a simple empirical equation to predict the time SOFC reaching steady state. The findings showed that the time of SOFC reaching steady state was related to the thermal properties of textures, flow structures, and operation conditions.

Brinkman et al. [3] discussed the effects of two different temperatures, 1,759 K and 2,057 K, on the conductivity of oxide ions. Mean square displacement of ions was firstly obtained, and Nernst–Einstein relation was then put in to acquire the conductivity of ions. Presently, the relation is commonly applied to obtain the conductivity of ions. In between 1999 and 2004, Yakabe et al. [4–6] preceded a series of flat SOFC value simulation analyses with package software ABAQUS and STAR-CD. The findings showed that recombination reactions would absorb heat at the entry of fuel in anode that resulted in the temperature in the region lower than it in the entry, but hereafter the temperature increased with the heat release of electrochemical reactions. The process of temperature rise and fall

J.-K. Kuo (✉) · J.-K. Wang
Department of Greenergy, National University of Tainan, Tainan, 70005 Taiwan, Republic of China
e-mail: jkkuo@mail.nutn.edu.tw

would cause electrolyte receiving a great amount of heat that further resulted in the damage of electrolyte texture. What is more, it was found that water gas shift reactions could help reduce the polarization of concentration in the cell, and the design of bipolar plate would affect the polarization of ohm and concentration.

Recknagle et al. [7] simulated the bipolar plate, designed by Yakabe et al. [5], in which the cell performance with different directions of gas flow was analyzed with numerical analyses in 2003. The findings showed that co-flow could make the cell present even temperature distribution. Then Suwanwarangkul et al. [8] numerically computed three concentration polarizations, as Dusty–Gas, Fick's, and Maxwell–Stefan, with numerical simulation. The analysis results displayed Dusty–Gas model the best, Fick's model the second, and Maxwell–Stefan model the worst. Nevertheless, Dusty–Gas model required numerical analyses to solve that were more complicated than the other two so that most research applied Fick's model to compute the concentration polarization.

Ackman et al. [9] applied fluent in computational fluid dynamics to precede the numerical simulation of SOFC, compare anode support and the current, temperature, and the concentration distribution of reactive gas in cathode-supported SOFC. The findings showed that, with the same operation conditions, anode-supported SOFC presented higher average current density, while cathode-supported SOFC appeared insufficient oxygen content below the rib of the flow channel due to the diffusion limitation of oxygen. In 2004, Aguiar et al. [10] simulated and analyzed the recombination of SOFC with 1D medium temperature and further compared the temperature distribution of co-flow and counterflow. The findings presented that the most loss of voltage in fuel cells was cathode activation polarization and anode activation polarization and ohmic polarization the next. Moreover, the flow field of counter-flow presented steep temperature gradient and uneven current density.

In 2005, Zhao and Virkar [11] utilized experimental data to develop flat anode-supported SOFC empirical equations with the parameters of electrolyte thickness, anode catalyst thickness, cathode support thickness, and anode support porosity. The findings showed that the maximum power density of SOFC was 1.8 W cm^{-2} at 800 °C. In 2006, Hussain and Dincer [12] simulated, with mathematical model, the effects of the various fuel gas compositions in flat anode-supported SOFC on cell performance. In 2007, Wang et al. [13] proposed the design of flat electrode-supported SOFC with omitted flow channel, which omitted the flow channel on the bipolar plate and established the flow channel in cathode/anode diffusion that current directly conducted from cathode/anode to the current collector. The findings presented that the design could effectively reduce the loss of concentration polarization.

Liu et al. [14] simulated and analyzed the operation conditions of various fuel flows in anode-supported SOFC, with package software Star-CD. The findings showed that the increase of fuel would help reduce fuel usage and increase power density. Moussa et al. [15] simulated the analyses of co-flow with 1D flat SOFC mathematical model and discussed the effects of hydrogen consumption on output power density of cells. The findings showed that when cathode and electrode were the supports, hydrogen consumption and power density would reduce, while hydrogen consumption and output power density would increase when anode was the support.

Mathematical model

SOFC is a generating plant transforming chemical energy into electric energy with electrochemical reactions. Figure 1 presents the schematic representation of SOFC structure. The operation principle is to transmit oxygen to cathode (air electrode) and at the same time be catalyzed into oxide ions, which are transmitted to anode (fuel electrode)

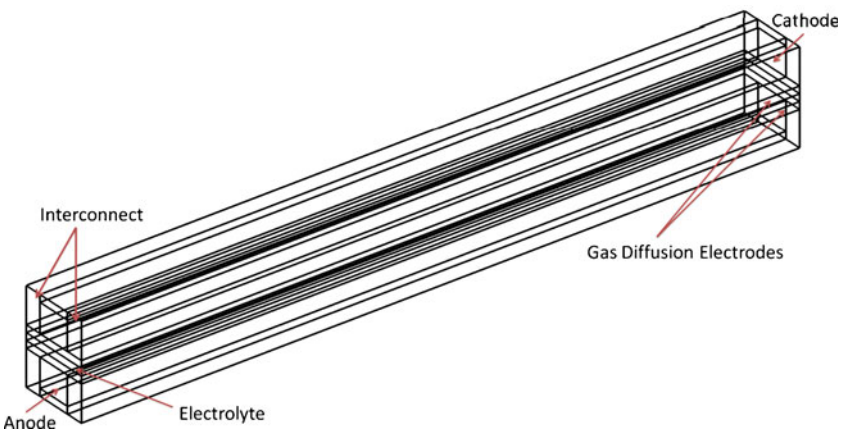

Fig. 1 Schematic representation of SOFC. **a** Flow field being counterflow; **b** flow field being co-flow

through solid electrolyte. Meanwhile, fuel gas, such as the hydrocarbon of hydrogen, methane, and anaeroic digestion gas, is transmitted into the anode end. Oxygen dissociated into oxide ions (O^{2-}) with electrochemical actions at cathode and transmitted to anode by the oxygen vacancy in the electrolyte. Then it is reacted with fuel gas to become water or CO_2. In the process of reactions, potential difference begins to generate between anode and cathode that result in electronic flow, as the action of cells. Electrochemical reactions can generate electric energy and water that is similar to transmit fuel (anode) and oxidant (cathode) into the region, where hydrogen and oxygen co-exist in the three-phase interface and result in electrochemical reactions.

Electrochemical model

When hydrogen is used as fuel, half electrochemical reaction in anode is as [16]

$$H_2 + O^{2-} \rightarrow H_2O + 2e^-, \quad (1)$$

half electrochemical reaction in cathode is as

$$O_2 + 4e^- \rightarrow 2O^{2-}, \quad (2)$$

and the entire electrochemical reaction is

$$2H_2 + O_2 \rightarrow 2H_2O \quad (3)$$

This study, based on solid oxide material in SOFC, discusses the mass transfer and current density distribution with various anode support thicknesses. The single cell in SOFC is selected as the research model which contains PEN plate with all-in-one structure of air electrode (cathode), solid electrolyte, and fuel electrode (anode), anode/cathode gas flow channel, both ends of gas transmission set as counterflow or co-flow, the entry fuel at anode being hydrogen, the entry fuel at cathode being oxygen, and bipolar interconnect, as Fig. 1.

In this model, anode is at the bottom layer and cathode at the top layer. Oxygen is transmitted from the entry of the flow channel at the top. With convection and diffusion, the gas enters gas diffusion and catalyst for electrochemical reactions to generate oxide ions (O^{2-}), which are transmitted to anode by electrolyte. The residual gas then flows out from the exit.

On the other hand, hydrogen is transmitted from the entry of the flow channel at the bottom. With convection and diffusion, the gas enters gas diffusion and catalyst where the fuel gas is electrochemically catalyzed and oxidized. The released electrons, after fuel gas oxidation, are transmitted to external circuits, and the oxide ions, from electrolyte, are transmitted into all-in-one activation interface. The residual gas then leaves from the exit.

Basic hypothesis

The electrolyte material in SOFC simulated in this study is applied to discuss the effects of various anode support thicknesses on mass transfer and current density distribution. In this case, before numerical simulation, the following hypotheses are made for the model to simplify the difficult of equations:

1. All mixture of gases is regarded as ideal gases.
2. The flow of gases is laminar flow and incompressible.
3. As fuel cells appear temperature change in themselves, the change of temperature is not taken into account, in order to simplify the question, and the fixed temperature is 1,073 K.
4. All diffusions and catalysts are with even texture and isotropic.
5. All reactants and resultants are in gaseous phase.

Governing equations

This study applies the equations of conservation of charge, conservation of mass, conservation of momentum, and conservation of concentration to describe the physical phenomena in SOFC. The conservation of charge of fuel cells occurs in the solid parts of electrolyte, catalyst, and gas diffusion, where the catalyst contains two solid textures of ionic conductors (electrolyte) and electronic conductors (catalyst) and the electrolyte and gas diffusion merely contain ionic conductors and electronic conductors, respectively. With Ohm's law, voltage balance in Yttria-stabilized zirconia (YSZ) separator and gas diffusion can be written as the following equations.

$$\nabla \cdot (-\sigma_{\text{elec}} \nabla \phi_{\text{electronic}}) = 0 \quad (4)$$

$$\nabla \cdot (-\sigma_{\text{ion}} \nabla \phi_{\text{ionic}}) = 0 \quad (5)$$

where σ_{elec} and σ_{ion} are the electronic conducting degree and the ionic conducting degree, respectively, and $\phi_{\text{electronic}}$ and ϕ_{ionic} the electronic phase potential energy and the ionic phase potential energy, respectively.

Regarding anode and cathode gas diffusion electrodes (GDE), current transmits from fuel electrodes to electrolyte in anode, while it transmits from electrolyte to air electrodes in cathode. With Ohm's law, the equation of the conservation of charge in gas diffusion is presented as

$$\nabla \cdot \left(-\sigma_{\text{electronic,eff}} \nabla \phi_{\text{electronic}}\right) = S_a i_{\text{ct}} \quad (6)$$

$$\nabla \cdot \left(-\sigma_{\text{ion,eff}} \nabla \phi_{\text{ionic}}\right) = S_a i_{\text{ct}} \quad (7)$$

where $\sigma_{\text{electronic,eff}}$ and $\sigma_{\text{ion,eff}}$ are effective electronic conductivity and equivalent ionic conductivity, respectively, S_a the specific surface region, and i_{ct} the local migrating current.

Describe the electrochemistry and transport phenomena of each component in the electrode with Bulter–Volmer equation.

$$i_{a,ct} = i_{0,a} x_{H_2} \frac{c_t}{c_{H_{2,ref}}} \left[\exp\left(\frac{0.5F}{RT}\eta\right) - \exp\left(\frac{-0.5}{RT}\eta\right) \right] \quad (8)$$

$$i_{c,ct} = i_{0,c} \left[\exp\left(\frac{0.5F}{RT}\eta\right) - x_{O_2} \frac{c_t}{c_{O_{2,ref}}} \exp\left(\frac{-0.5}{RT}\eta\right) \right] \quad (9)$$

where, $i_{a,ct}$ and $i_{c,ct}$ are the local migrating currents in anode and cathode, respectively, $i_{0,a}$ and $i_{0,c}$ the exchange current densities of the anode and cathode, x_{H_2} and x_{O_2} the mass fractions of hydrogen and oxygen, c_t the molarity, F the Faraday's constant, R the gas constant, and T the temperature.

Equation of conservation of mass

The equation of conservation of mass that fluid flows through porous electrode and gas flow channel is also called continuity equation.

$$\frac{\partial}{\partial t}(\varepsilon\rho) + \nabla \cdot (\varepsilon\rho u) = S_m \quad (10)$$

where ρ and u are the average density and speed (vector) of the fluid. In addition to catalyst, source term S_m presents zero in the rest regions. In previous equation, the porosity of the porous media ε is incorporated to be applicable in porous regions including gas diffusion and catalyst. Besides, setting suitable porosity in each sub-region could help the equation applicable in full field fuel cells.

Equation of conservation of momentum

The equation of conservation of momentum that fluid flow through gas flow channel is presented as

$$\rho(u \cdot \nabla)u = -\nabla P + \mu\nabla^2 u + \frac{2}{3}\mu\nabla(\nabla \cdot u) \quad (11)$$

$$\nabla(\rho u) = Q \quad (12)$$

where P is the pressure and μ the dynamic viscosity.

The equation of conservation of momentum that fluid flow through porous gas diffusion electrode is presented as

$$\left(\frac{\mu}{\kappa} + Q\right)u = -\nabla P + \frac{\mu}{\varepsilon}\nabla^2 u + \frac{2}{3}\mu\nabla(\nabla \cdot u) \quad (13)$$

$$\nabla(\rho u) = Q \quad (14)$$

ε is the porosity of porous media, standing for the ratio of porosity volume and entire capacity in porous media. The source term Q is the quantity that the gas is consumed or generated from electrochemical reactions.

$$Q = \sum\nolimits_i S_a \frac{i_{ct,i} M_i}{n_i F} \quad (15)$$

where $i_{ct,i}$ is the local migrating current of the gas element i and n_i the number of electronic reactions. Both gas diffusion and catalyst are porous media that Brinkman equation is more appropriate, as the source term in Brinkman equation can apply Darcy's law, which also describes the momentum balance in porous electrodes.

$$u = -\frac{\kappa}{\mu}\nabla P \quad (16)$$

k is the permeability of the porous media standing for the porosity volume that porous media occupy in unit volume. When k is large, the Darcy's viscosity is neglected so that the equation presents the model of Navier–Stokes equation.

Equation of conservation of concentration

In this study, there are two gas elements, namely H_2 and H_2O, in anode and three gas elements, namely O_2, H_2O, and N_2, in cathode. The conservation of concentration of each gas element can be presented with Maxwell–Stefan equation.

$$\nabla \cdot \left[w_i\rho u - \rho w_i \sum\nolimits_{j=1}^{k} D_{ij} \left\{ \frac{M}{M_j}\left(\nabla w_j + w_j \frac{\nabla M}{M}\right) + \left(x_j - w_j \frac{\nabla P}{P}\right) \right\} \right] = S_i \quad (17)$$

where w_i stands for the mass fraction of gas element i and D_{ij} the binary diffusion coefficient between the gas elements of i and j. The binary diffusion coefficient between the two gas elements can be obtained with dynamics theory [17].

$$D_{ij} = 1.8583 \times 10^{-7} \frac{T^{1.5}\left(\frac{1}{Mw_i} + \frac{1}{Mw_j}\right)}{P\Omega_D \sigma_{ij}} \quad (18)$$

Ω_D is the collision integral and σ_{ij} the diameter of the molecular collisions. The source term S_i stands for the quantity that the gas element i is consumed or generated from electrochemical reactions. In open flow channels, the source term is set zero, while it is given by the velocity of electrochemical reactions in GDE. The calculation of charge transfer current density is based on Faraday's law.

$$S_i = v_i \frac{i_{ct,i} M_i}{n_i F} \quad (19)$$

where v_i is the stoichiometric coefficient, n_i the number of electronic reactions, w_i the mass fraction of gas element i,

and x_i the mole fraction of gas element i. The relation of w_i and x_i is shown as [18]

$$x_i = w_i \cdot \frac{M}{M_i} \tag{20}$$

where M stands for the molecular weight of the total mixed gas and M_i the molecular weight of gas element i. The relation of M_i and M is presented as

$$M = \sum_{i=1}^{k} M_i \cdot x_i \tag{21}$$

Since fluid is the ideal gas of various gas mixture, the density of the mixed gas ρ is presented as

$$\rho = \frac{PM}{RT} \tag{22}$$

where ρ is the density, P the pressure, R the universal gas constant, and T the temperature.

Boundary condition

Aiming at the boundary condition of the single cell model in SOFC, this study mainly contains the PEN plate (membrane electrode assembly) with all-in-one structure of air electrode (cathode), solid electrolyte (YSZ film), and fuel electrode (anode), anode/cathode gas flow channels, and bipolar interconnect.

Solid electrolyte (YSZ film)

Aiming at the equilibrium equation of ionic current, oxide ions are transmitted in between fuel/air electrodes and electrolyte surface in this study. The rest surfaces beyond solid electrolyte are set as ionic insulator, with the boundary condition as

$$n_i \cdot \left(-\sigma_{\text{ion}} \nabla_{\text{ionic}}\right) = 0 \tag{23}$$

Anode/cathode gas flow channel

The boundary condition in the equilibrium equation of mass and concentration, in this study, also considers the regions included in electrode. In addition to the entry and exit being with mass fractions, the rest boundaries are set as insulation condition with the boundary condition as

$$n_i \cdot \left(-\sigma D_{ij} \nabla w_i + \rho u w_i\right) = 0 \tag{24}$$

The boundary condition of the entry is set with gas mass fraction, as

$$w_i = w_{i,0} \tag{25}$$

The boundary condition of the exit is set with gas mass fraction, as

$$n_i \cdot \left(-\sigma D_{ij} \nabla w_i\right) = 0 \tag{26}$$

Regarding the boundary condition of dynamic balance equation, despite the boundary conditions of the entry and the exit, the rest boundaries are set as no-slip, with the boundary condition as

$$n_i \cdot \left(-\sigma D_{ij} \nabla w_i + \rho u w_i\right) = 0 \tag{27}$$

The pressure boundary condition of the entry of the gas flow channel is

$$P = P_{\text{atm}} + \mathrm{d}P \tag{28}$$

while the pressure boundary condition of the exit of the gas flow channel is

$$P = P_{\text{atm}} \tag{29}$$

Numerical method

In this study, the simulations are performed using the commercial COMSOL software package, which discretizes the mass, momentum, gas diffusion electrodes, and species concentration equations using the finite-volume semi-implicit method for pressure-linked equations consistent method [19]. In the simulations, it is assumed that the inlet section of the channel is fully developed hydrodynamically. Hence, a fully developed velocity profile for rectangular ducts is imposed. Additionally, a forced convection regime is imposed within the computational domain, and the Navier–Stokes equations are solved under laminar assumptions. Prior to the simulations, a parametric study was performed to identify a suitable grid mesh for accurately modeling the thermal and velocity gradients near the walls in order to provide detailed insights into the electrochemical reaction and mass transport phenomena in the proton exchange membrane fuel cells. A spatial resolution of 858×400 meshes was found to be sufficient, with a fine mesh size used throughout the computational domain. In the simulations, the iterative computations were terminated once the value of the residues fell to less than 10^{-6}. The computations were performed using a PC with a 3.2-GHz Intel Pentium 4 CPU, 2 GB DDR RAM, and the Windows XP operating system.

Results and discussions

This study aims to discuss the effects of electrolyte material in SOFC on the cell performance of SOFC, where the flow

fields are set counterflow and co-flow and the adjusted parameters include anode support thickness, electric potential, and porosity; to discuss the effects of various changes of voltage and concentration on the mass transfer, current density distribution, I–V curve, and power density of SOFC; and finally to analyze and compare the features of the numeric simulation.

Counterflow and co-flow

The design of flow channels has great influence on fuel cell performance. Besides the configurations of flow channels being important, this study will discuss the effect of gas flow on the cell performance of SOFC. Figure 2 presents the various flow fields of SOFC. The cell module is set counterflow and co-flow, where counterflow is the hydrogen in anode and the air in cathode is the reverse flow direction; contrarily, the flow directions of co-flow are the same.

Effect on hydrogen mass fraction

Figure 3 shows the comparison of hydrogen mass fraction between the flow fields of counterflow and co-flow, where the hydrogen mass fraction of co-flow is at $L_{channel}$=0.005 m (X=0.005 m) that gas is evenly distributed in gas diffusion electrode and helpful for the electrochemical reactions on the catalyst, while the hydrogen mass fraction of counterflow presents large concentration change among flow channels that the electrochemical reactions on the catalyst are poorer than co-flow.

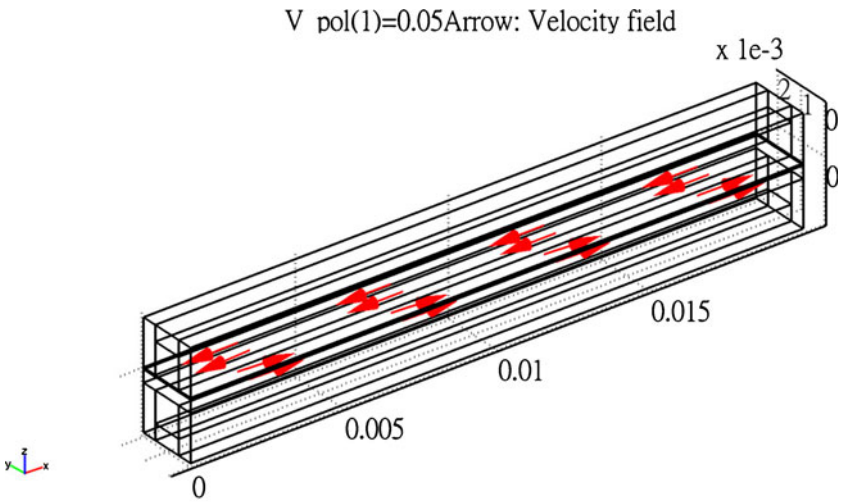

(a) Flow field being counter-flow

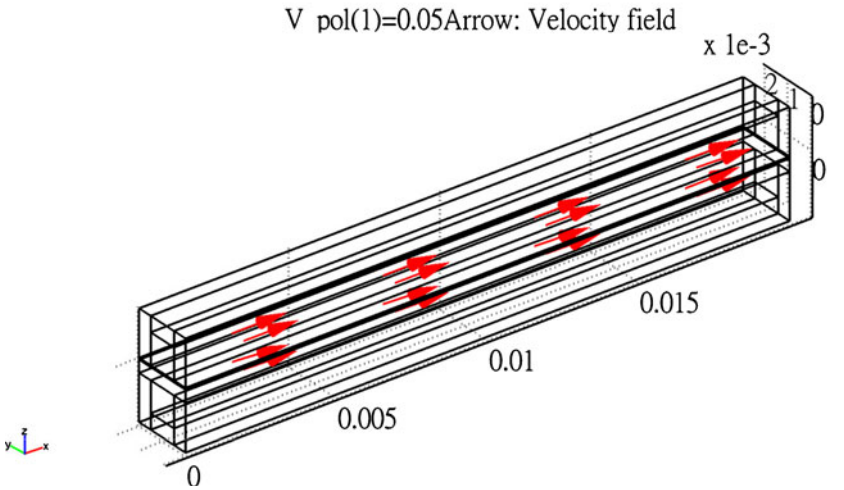

(b) Flow field being co-flow

Fig. 2 Various flow fields of SOFC

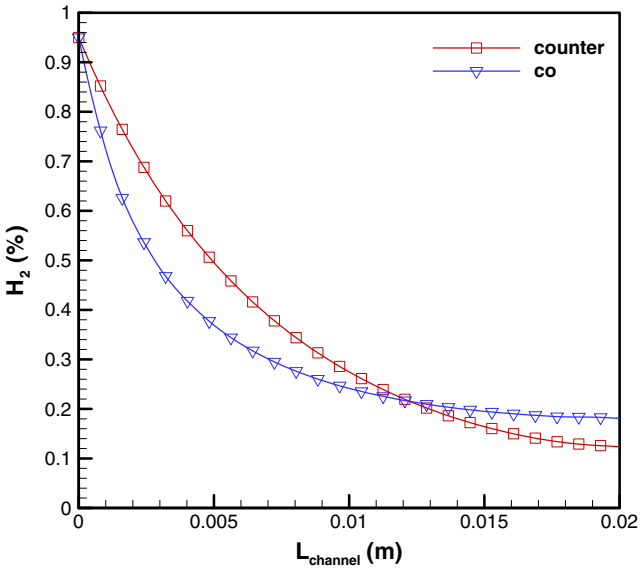

Fig. 3 Distribution of the effects of counterflow and co-flow on hydrogen mass fraction

Effect on oxygen mass fraction

From Fig. 4, the difference of concentration distribution in the flow channels between counterflow and co-flow to oxygen mass fraction is not large. Nonetheless, since the electrochemical reaction of oxygen generates oxide ions (O^{2-}), which are transmitted to anode through electrolyte and imported to three-phase interface reaction to generate current density, the concentration distribution of oxygen cannot be poor. To improve the insufficiency of oxygen concentration distribution and current density distribution, oxygen flow is increased to enhance the mass transfer of oxygen.

Effect on SOFC performance

From the analyses of hydrogen mass fraction, the concentration distribution of co-flow hydrogen mass fraction is more even than it of counterflow in the flow channel so that hydrogen can be evenly distributed in the catalyst with better electrochemical reactions. However, the concentration distribution of oxygen is not worse either, as the increase of oxygen flow can, with both co-flow and counterflow, help defer concentration polarization in the cell and further help promote the overall performance of fuel cells. As shown in Figs. 5 and 6, co-flow is likely to obtain better I–V curve and the output power density is better than counterflow.

The comparison of hydrogen mass fraction distribution between diffusion and flow channels

Figure 7 presents the concentration distribution of hydrogen in anode of SOFC with various anode support thicknesses (Ni/YSZ). Hydrogen reacts by diffusing from the flow channel to gas diffusion electrode. In the figure, hydrogen would be consumed by electrochemical reactions, and the concentration distribution of hydrogen would reduce with the direction hydrogen flows in the flow channel, as hydrogen continuously precedes an electrochemical reaction that results in the consumption of hydrogen.

Figure 8 illustrates the comparison of various anode support thicknesses with co-flow. In the figure, the curve

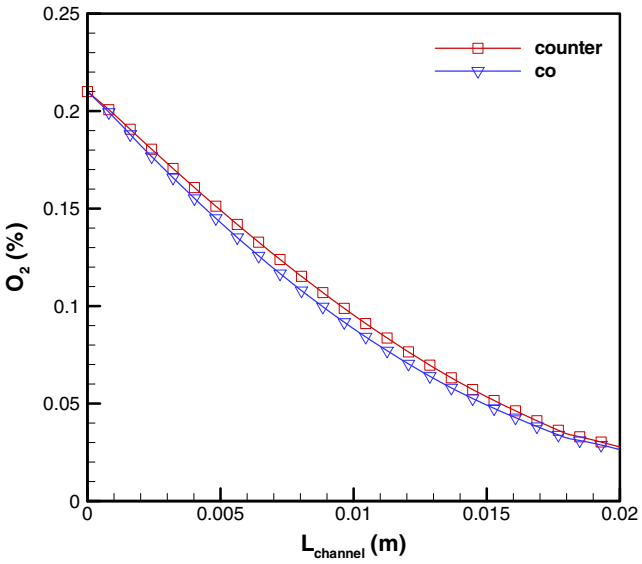

Fig. 4 Distribution of the effects of counterflow and co-flow on oxygen mass fraction

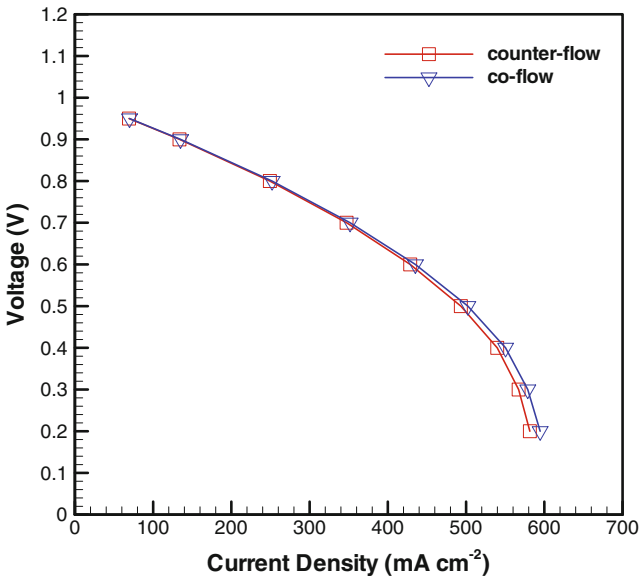

Fig. 5 Effect of various flow fields on I–V curve

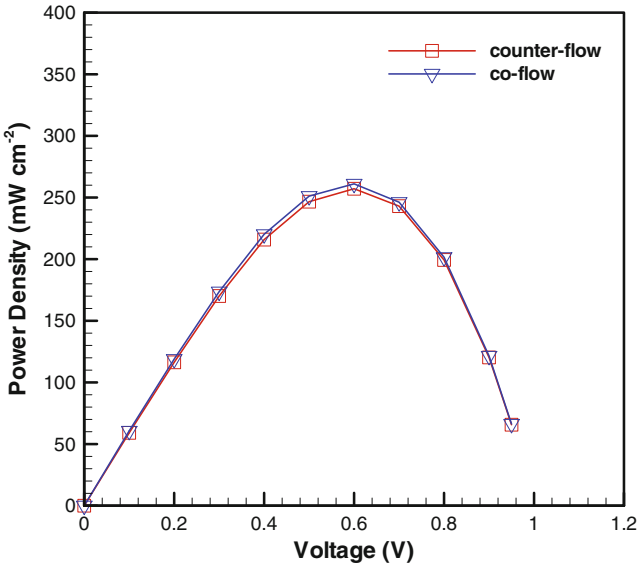

Fig. 6 Effect of various flow fields on P–V curve, **a** 400 μm, **b** 600 μm, **c** 800 μm, **d** 1,000 μm

with ruffle waves appears at the direction when hydrogen approaching the exit of the flow channel, as in the process of hydrogen electrochemical reactions, un-reacted residual gas distributes in the flow channel and flows toward the exit that the hydrogen electrochemical reactions in catalyst becomes poor, when the operation voltage rises and the residual gas in the flow channel increases, as well as the pressure difference in the entry of the flow channels results in the curve with wave peaks appearing at the exit.

The comparison of oxygen concentration distribution between diffusion and flow channels

Figure 9 illustrates the distribution of oxygen mass fraction with various flow fields between cathode porous electrodes and the flow channel. Similar to hydrogen, oxygen begins electrochemical reactions, once it enters the flow channel, and is consumed with the electrochemical reactions that the oxygen concentration distribution would gradually decreased along the flowing direction. It is found in the figure that oxygen diffuses from the flow channel to gas diffusion electrodes and reaches catalyst for reactions that the closer it reaches the catalyst, the lower the oxygen concentration becomes.

This study does not discuss the effects of changing cathode support thicknesses on SOFC performance, but the oxygen transmission in SOFC cathode is related to mass transmission. From the principles of SOFC, oxygen electrochemical reactions would generate oxide ions (O^{2-}) which are transmitted to anode through electrolyte and imported to three-phase reactions to generate current density so that the oxygen concentration distribution cannot

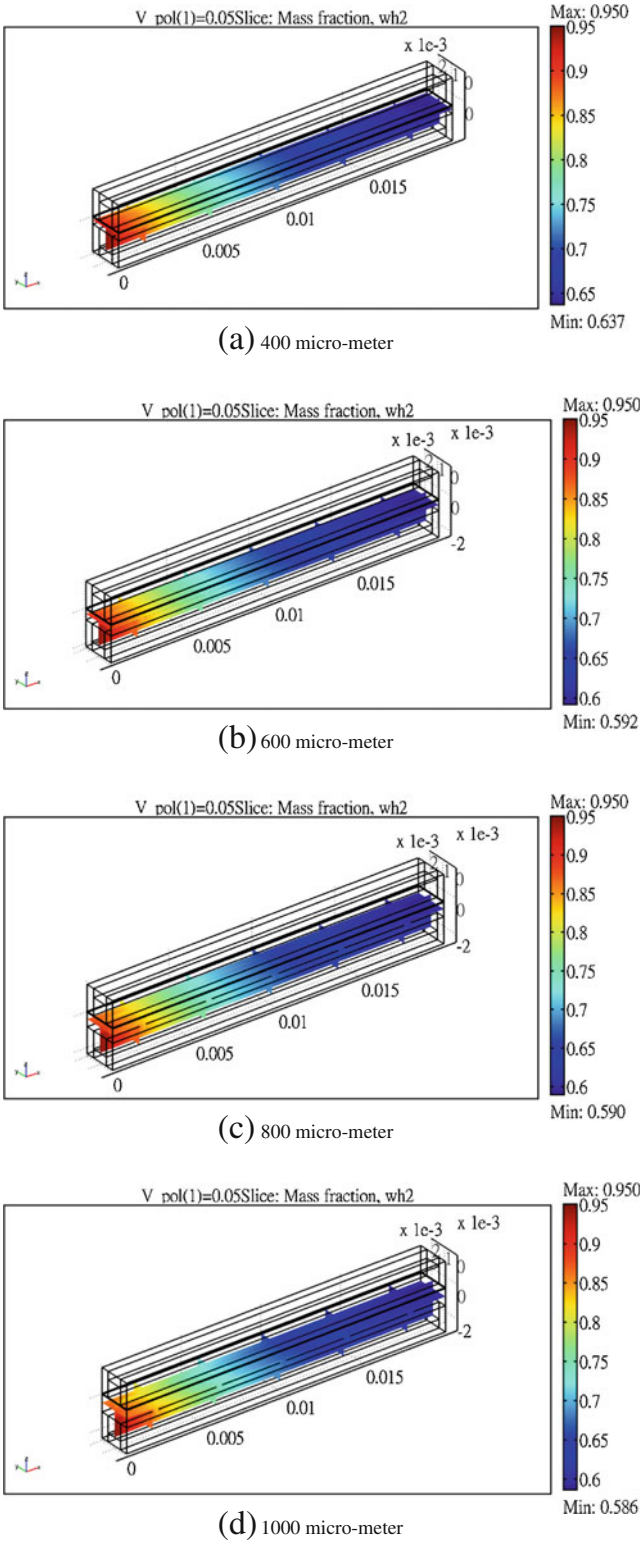

Fig. 7 Anode hydrogen concentration distribution in SOFC with various anode support thicknesses (Ni/YSZ)

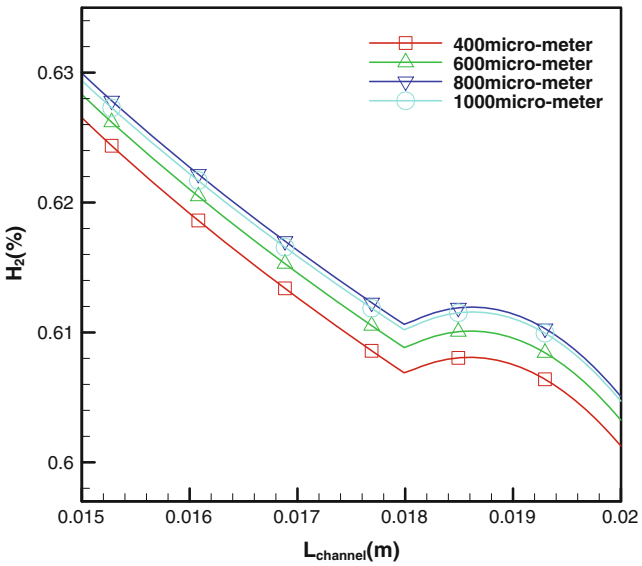

Fig. 8 Hydrogen concentration distribution with various anode support thicknesses

be poor. To improve the insufficiency of concentration distribution and current density distribution, oxygen flow can be increased to promote oxygen mass transfer.

Effect on SOFC performance

According to the comparison of hydrogen mass fraction consumption in Table 1, the larger the anode support thickness, the more consumption of hydrogen that the electrochemical reactions in catalyst become well, and the hydrogen mass fraction remained in the flow channel is less. Figure 10 presents I–V curve of various anode support thicknesses, where the consumed hydrogen mass fraction is the most at the anode support thickness 1,000 μm that allows fuel cells staying in high current state and timely reacts to electrode surface to maintain high charge exchange. On the other hand, when anode support thickness is 400 μm, the consumption of hydrogen mass fraction is less and the electrode surface could not remain proper

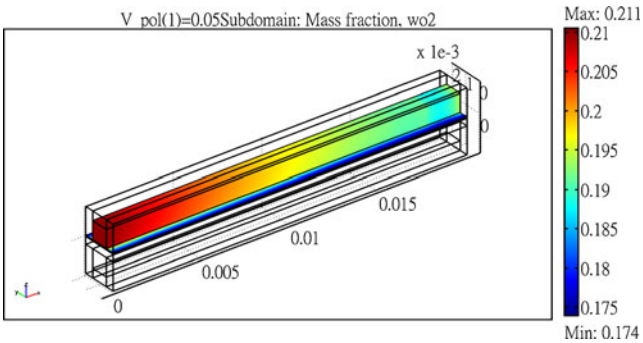

Fig. 9 Oxygen concentration distribution in cathode flow channels

Table 1 Consumption of hydrogen mass fraction with various anode support thicknesses

Thickness (μm)	Hydrogen mass fraction at the entry (%)	Hydrogen mass fraction at the exit (%)	Consumed hydrogen mass fraction (%)
400	0.95	0.637	0.313
600	0.95	0.592	0.358
800	0.95	0.590	0.360
1,000	0.95	0.586	0.364

hydrogen so that higher concentration changes resulted. Figure 11 shows the enlarged comparison of various anode support thicknesses, where the current density distribution at anode support thickness 1,000 μm is better than other three different anode support thicknesses.

Effect on various potential

In the design of SOFC, the voltage and current density distributions in flow field is crucial [20]. According the various anode support thicknesses correlate with hydrogen concentration distribution. The consumption of various voltages to reactant mass fraction is further discussed in this chapter to obtain the effect of reactant consumption on current density and SOFC performance.

Effect of various voltages on hydrogen mass fraction

With the effect of output voltage being 0.95, 0.7, and 0.5 V on hydrogen mass fraction, hydrogen mass fraction among

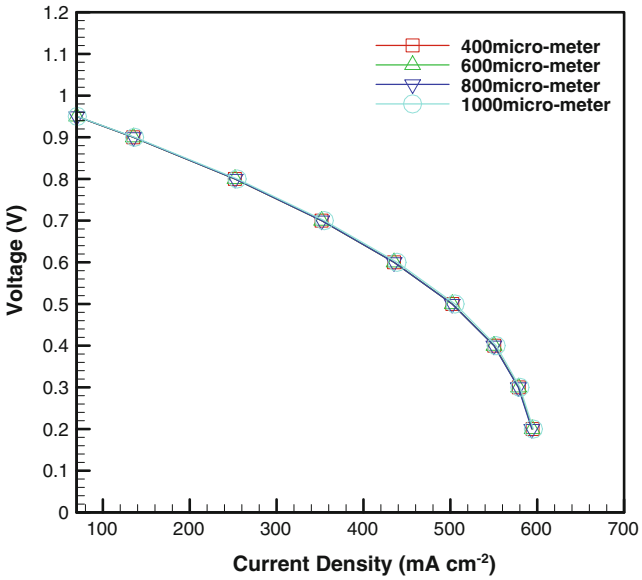

Fig. 10 I–V curve with various anode support thicknesses

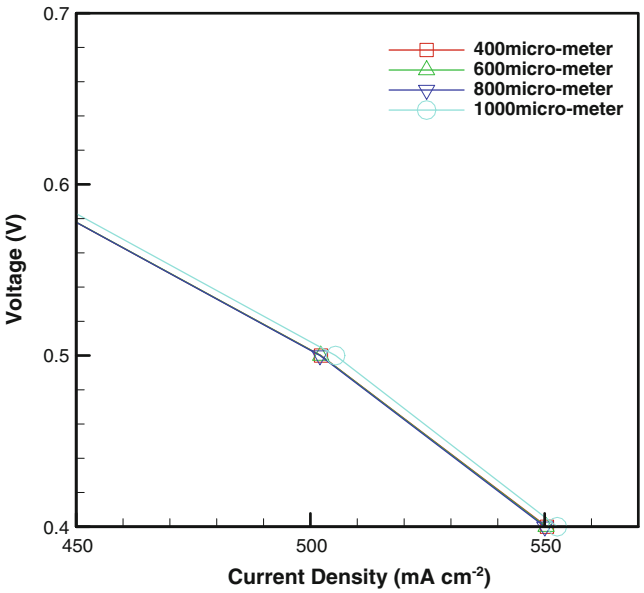

Fig. 11 Enlarged distribution of I–V curve with various anode support thicknesses

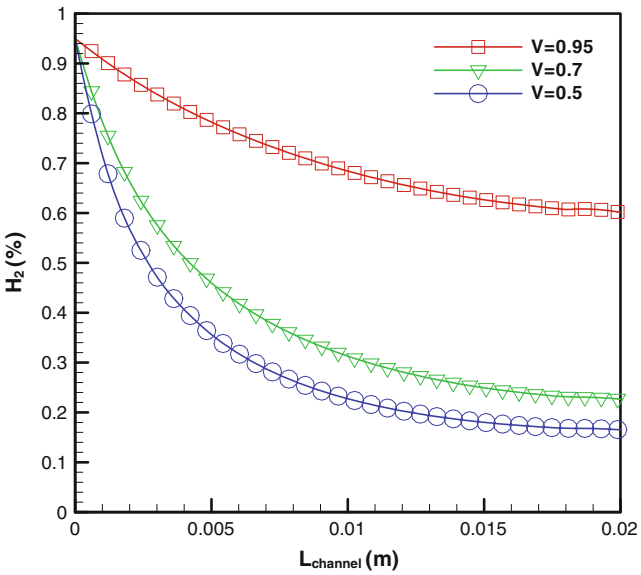

Fig. 13 Distribution of oxygen mass fraction consumption with various voltages

the flow channel distribution and current density distribution with various voltages is discussed. Figure 12 presents the effect of operation voltage on hydrogen mass fraction, and Fig. 13 shows the distribution of various operation voltages to the consumption of hydrogen mass fraction. It is found from the figures that electrochemical reactions are gentle when the operation voltage is 0.95 V so that the hydrogen concentration at the entry and the exit does not appear too much difference. However, when the operation voltage is 0.5 V, the electrochemical reactions are violent and the consumption of hydrogen is the most that the SOFC current density reaches a better value in the three voltages.

Effect of various voltages on oxygen mass fraction

Figure 14 shows the effect of operation voltage on oxygen mass fraction. Similar to oxygen, with the operation voltage being 0.95, 0.7, and 0.5 V, the consumption of oxygen mass fraction is the most when the operation voltage is 0.5 V (Fig. 15).

Effect of various porosities

This chapter aims at porosity features of the inner texture of electrolyte material in SOFC, such as porosity (ε) and tortuosity (τ). The electrode and catalyst in fuel cells should have certain porosity so that the vacancies are associated to allow reactive gas flowing in the electrode. In this study, the porosity being 0.3, 0.5, and 0.7 and the tortuosity 4.5 are selected to analyze the effect on SOFC performance. Figures 16 and 17 present the effects of various porosities on I–V curve and power density in SOFC. According to the above curves, it is found that the fuel cell performance can be effectively enhanced with larger ratio of porosity and tortuosity [7] that high porosity presents the vacancies in porous medium and can be effectively associated and allow the gas flowing through. From the analyses of the three

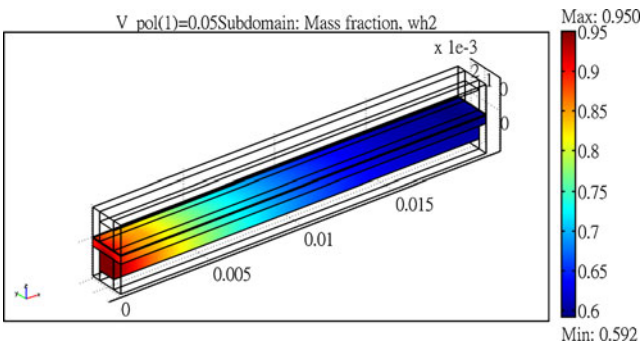

Fig. 12 Effect of operation voltage on hydrogen mass fraction

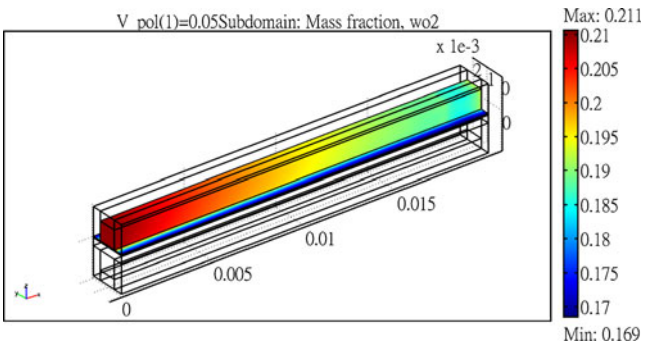

Fig. 14 Effect of operation voltage on oxygen mass fraction

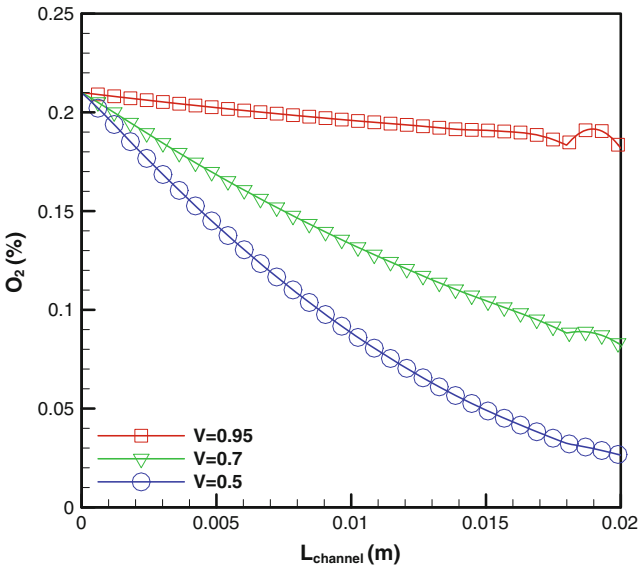

Fig. 15 Distribution of oxygen mass fraction consumption with various voltages

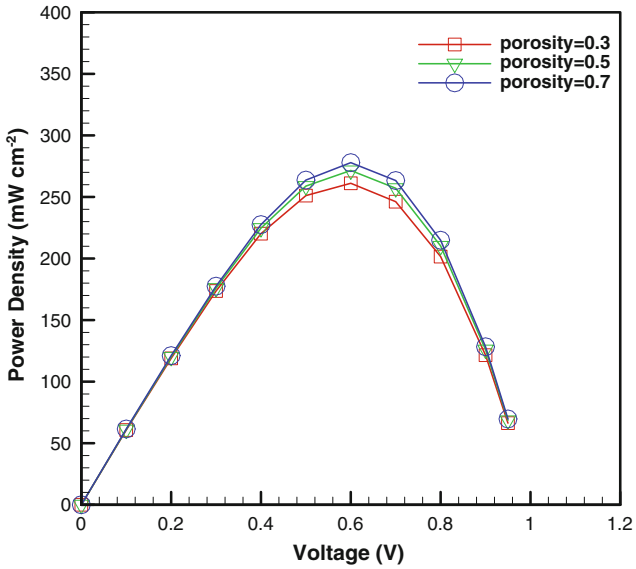

Fig. 17 Effect of various porosities on SOFC power density

porosities, current density presents better distribution when the porosity is 0.7, in comparison with other ratios of porosity and tortuosity. Regarding power density, the output power of SOFC reaches the best performance when the output voltage is 0.6 V.

Conclusions

This study applies COMSOL Multiphysics to establish 3D SOFC model and analyzes mass transfer features in solid oxide material. The features include (1) various flow fields, (2) operation voltage, (3) the design with various electrode supports (anode support), and (4) various porosities. With these parameters, the effects on the mass transfer and cell performance of electrolyte material in SOFC are further discussed. The conclusions are shown as follows:

1. With the analyses of various flow fields, the findings show that hydrogen mass fraction with co-flow can be evenly distributed in electrolyte material that the overall performance of co-flow is better than it of counterflow.
2. With the effect of various potentials, the best power density is obtained when co-flow is at the operation voltage 0.6 V.
3. Regarding concentration analyses, oxygen is more in cathode flow channel that high concentration oxygen appears in the flow channel and more oxygen is transmitted to the catalyst. In this case, with the oxygen concentration on the high catalyst surface, the SOFC performance is further promoted.
4. Regarding the analyses of various porosities, the fuel cell performance can be effectively promoted with larger ratio of porosity and tortuosity. According to the analyses of I–V curve and power density curve, the ratio with tortuosity reaches the maximum when porosity is 0.7.

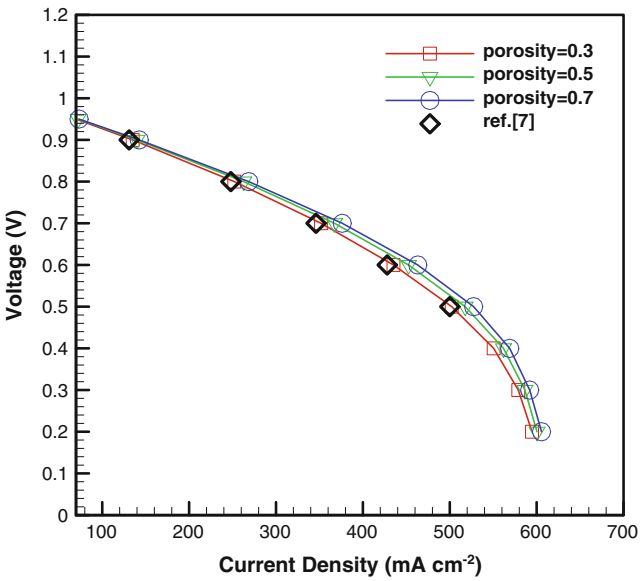

Fig. 16 Effect of various porosities on SOFC I–V curve

Nomenclature

C	Mass fraction (moles per cubic meter)
C_{H_2}	Hydrogen concentration (moles per cubic meter)
C_{O_2}	Oxygen concentration (moles per cubic meter)
D_{ij}	Maxwell–Stefan diffusion coefficient (square meters per second)

E	Cell voltage (volts)
F	Faraday constant (96,487 C mol^{-1})
H_2	Hydrogen
H_2O	Water
i	Current density (milliamperes per square centimeter)
$i_{ct,i}$	Local migrating current
$i_{0,a}$	Anode exchange current density (milliamperes per square centimeter)
$i_{0,c}$	Cathode exchange current density (milliamperes per square centimeter)
M	Molecular weight (kilograms per mole)
N_2	Nitrogen
n_i	Number of electronic reactions
O_2	Oxygen
P	Pressure (atmosphere)
S	Source term
R	Universal gas constant (8.314 J mol^{-1} K^{-1})
S_a	Body surface area
T	Temperature (kelvin)
u	Average velocity
v	Volume fraction
w	Mass fraction

Greek symbols

α	Charge transfer rate
ε	Porosity
ϕ	Phase potential (volts)
κ	Permeability
η	Overpotential (volts)
χ	Mole fraction
μ	Viscosity of flow (square meters per second)
ρ	Density (kilograms per cubic meter)
σ	Ionic conductivity (per ohm per meter)
τ	Tortuosity

Subscripts

eff	Effective
a	Anode
act	Activation
c	Cathode
conc	Concentration
i	i component
j	j component
ohm	Ohm impedance
ref	Reference

Acknowledgments This study was sponsored by the Institute of Nuclear Energy Research under contract no. 992001INER045.

References

1. Achenbach E (1994) Three-dimensional and time-dependent simulation of a planar solid oxide fuel cell stack. J Power Sources 49:333–348
2. Achenbach E (1995) Response of a solid oxide fuel cell to load change. J Power Sources 57:105–109
3. Brinkman HW, Briels WJ, Verweij H (1995) Molecular dynamics simulations of Yttria-stabilized zirconia. Chem Phys Lett 247:386–390
4. YaKabe H, Hishinuma H, Uratani M, Matsuzaki Y, Yasuda I (1999) Evaluation and modeling of performance of anode-supported solid oxide fuel cell. J Power Sources 86:423–431
5. Yakabe H, Ogiwara T, Hishinuma M, Yasuda I (2001) 3-D model calculation for planar SOFC. J Power Sources 102:144–154
6. Yakabe H, Sakurai T (2004) 3D simulation on the current path in planar SOFCs. Solid State Ionics 174:295–302
7. Recknagle KP, Williford RE, Chick LA, Rector DR, Khaleel MA (2003) Three-dimensional thermo-fluid electrochemical modeling of planar SOFC stacks. J Power Sources 113: 109–114
8. Suwanwarangkul R, Croiset E, Fowler MW, Douglas PL, Entchev E, Douglas MA (2003) Performance comparison of Fick's, dusty-gas and Stefan–Maxwell model to predict the concentration overpotential of a SOFC anode. J Power Sources 122:9–18
9. Ackman T, de Haart LGJ, Lehnert W, Stolten D (2003) Modeling of mass and heart transport in planar substrate type SOFCs. J Electrochem Soc 150:A783–A789
10. Aguiar P, Adjiman CS, Brandon NP (2004) Anode supported intermediate temperature direct internal reforming solid oxide fuel cell. I: model-based steady-state performance. J Power Sources 138:120–136
11. Zhao F, Virkar AV (2005) Dependence of polarization in anode-supported solid oxide fuel cells on various cell parameters. J Power Sources 141:79–95
12. Hussain MM, Li X, Dincer I (2006) Mathematical modeling of planar solid oxide fuel cells. J Power Sources 161:1012–1022
13. Wang Y, Yoshiba F, Watanabe T, Weng S (2007) Numerical analysis of electrochemical characteristics and heat/species transport for planar porous-electrode-supported SOFC. J Power Sources 170:101–110
14. Liu HC, Lee CH, Shiu YH, Yi R, Yan WM (2007) Performance simulation for an anode-Supported SOFC using Star-CD code. J Power Sources 167:406–412
15. Moussa HB, Zitouni B, Oulmi K, Mahmah B, Belhamel M, Mandin P (2009) Hydrogen consumption and power density in a co-flow planar SOFC. J Hydrogen Energy 34:5022–5031
16. EG, G Technical Services Inc. (2004) Fuel cell handbook (the seventh edition). U.S. Department of Energy, Morgantown
17. Naveed A, Stephen PD, Daniel L, Kevin K (2009) A three-dimensional numerical model of a single-chamber solid oxide fuel cell. J Hydrogen Energy 34:8645–8663
18. Shi Y, Cai NS, Li C (2007) Numerical modeling of an anode-supported SOFC button cell considering anodic surface diffusion. J Power Sources 164:639–648
19. Patankar SV (1980) Numerical heat transfer. Hemisphere, Washington, DC
20. Kuo JK (2010) Numerical investigation into thermofluidic and electrochemical characteristics of tubular-type SOFC. Fuel Cells 10:463–471